Performance Optimization of Solar Cells
Characterization of Buried Interfaces in CIGSSe with LEAP®

Application Note #APT-10

Solar is the world's fastest-growing form of renewable energy, with net solar energy generation increasing by an average of 8.3% per year. Although solar power conversion efficiency for laboratory cells ranges from 20.5%, for thin film technology, to 46%, for hetero-junction technology, these average figures drop to 15% and 21% respectively for commercially available photovoltaic modules [1]. Consequently, many research groups invest time and energy developing new material combinations aimed at reducing environmental issues such as chemical toxicity from standard buffer materials, as well as lowering production costs and energy payback times.

A promising alternative to the widely used Si and CdTe photovoltaics is Cu(In,Ga)(S,Se)2 (CIGSSe)-based thin film solar cells [2]. The thin film stack active layer consists of a glass substrate, Mo back contact, p-CIGSSe absorber layer, n-buffer, and an i-ZnO + n-ZnO+ Ni/Al grid (front contact). The 20 to 60 nm thick buffer is critical to device performance, because together with the absorber layer, it forms the p/n-junction necessary for charge separation.

Researchers have shown that buffer layers such as In_2S_3, ZnS, or even mixed In_2S_3/ZnS are good choices for obtaining a high performance solar device. This mixed ZnS-In_2S_3 buffer layer shows better open circuit voltage (Voc) and efficiency compared to pure In_2S_3 buffer. These improvements are explained by defect passivation by the ZnS Nano-Dots (NDs) and charge carrier transport via the In_2S_3 point contacts.

Atom Probe Tomography (APT) played a critical role in elucidating why the device containing the mixed buffer provided higher efficiency. In the ZnS NDs/In_2S_3 data shown in Figure 2, Zn was found in the first monolayers of the absorber layer, which is highlighted in grey. This may lead to a downward band bending at the surface. This configuration is very stable due to Fermi level pinning at the conduction band, as observed for a Cd buffer in the CIGSSe structure and reduces the recombination rate at the interface.

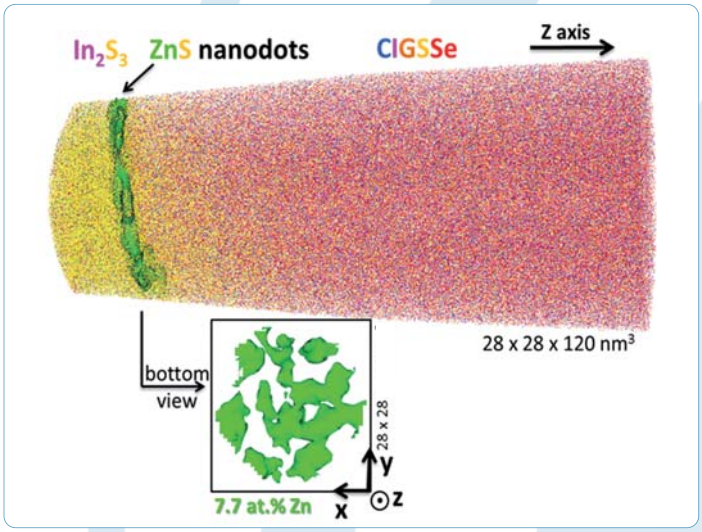

Figure 1:
Atom probe tomography 3D map showing the distribution of In (pink), S (yellow), Zn (light green), Cu (blue), Ga (orange), and Se (red).
The presence of the ZnS nanodots at the In_2S_3/Cu(In,Ga)Se_2 interface is clearly shown in the bottom view element envelope

Figure 2:
Proximity histogram across In_2S_3/ZnS/CIGSSe using an iso-concentration threshold value of 40 at.% sulfur.

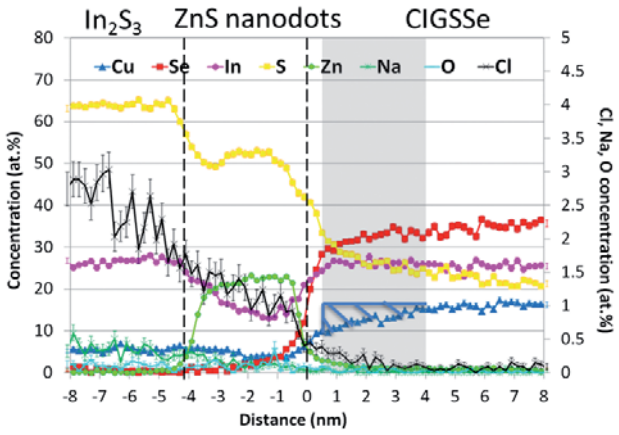

[1] Photovoltaics Report, Fraunhofer institute for solar Energy Systems, PSE AG, 6 June 2016
[2] Oana Cojocaru-Mirédin et al., Progress in Photovoltaics: Research and Applications, 2015; 23:705–716, DOI: 10.1002/pip.2484

AN#APT-10 - CIGSSe - March 17

Three Steps to 3D Nanoscale Analysis
An Introduction to Atom Probe Tomography

Step 1: Specimen Preparation

An atom probe specimen usually has a nanoscale region of interest (ROI) requiring both 3D compositional imaging and analysis. The sample is formed into a needle shape containing the ROI. Common APT specimen preparation methods using electropolishing or a Focused Ion Beam system (FIB) are very similar to TEM methods except instead of forming a thin sheet, a needle shaped sample is desired. At the right, standard FIB liftout and mounting of a specimen (figures 1 through 3) and then sharpening the sample with the ROI left at the very apex (4 and 5). In 6, a wire geometry sample is being electropolished.

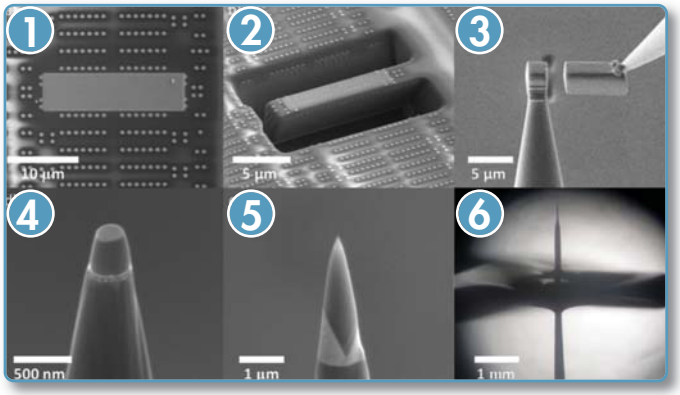

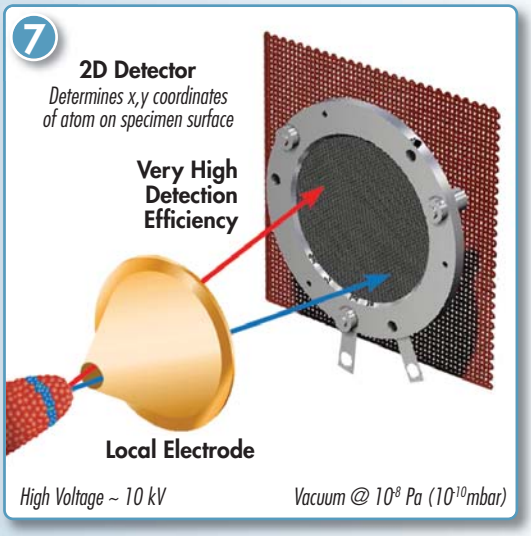

Step 2: Data Collection

An atom probe produces images by field evaporating atoms from a needle-shaped specimen and projecting the resultant ions onto a detector 7.

A high magnification results from the ~ 80nm tip being projected onto an 80mm detector resulting in a magnification of approximately 10^6.

An atom probe identifies atoms by their mass-to-charge-state ratio *(m/n)* using time-of-flight mass spectrometry. Charge state, *n*, is typically 1 to 3.

The specimen is held at approximately 50K to reduce surface diffusion during the experiment. The high electric field results in 100% ionization and the high speed detector is capable of measuring up to 80% of the collected ions, independent of ion mass.

Step 3: Data Visualization and Analysis

Examples of data output are illustrated by a slice of a 3D atom map of a transistor† 8, and a dopant composition profile‡ 9. The image shows the positions of individual atoms (oxygen is red and boron is blue) in the transistor with subnanometer resolution. From the reconstructed data set many types of useful analyses are possible. These include 3D visualization, 2D atom mapping 8, 1D depth profiling and line scanning 9, as well as mass spectra and compositional analysis from user-selected volumes.

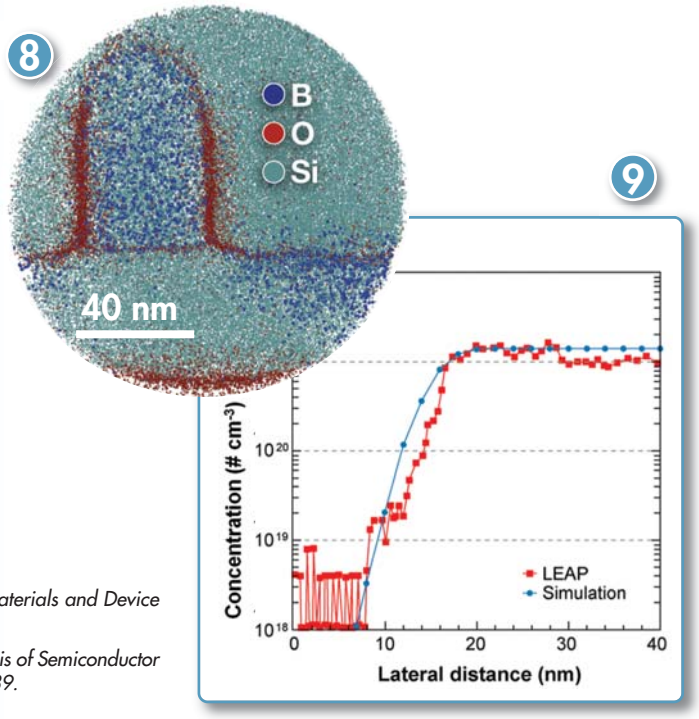

† *Lauhon, L. J. et al, MRS Bulletin "Atom Probe Tomography of Semiconductor Materials and Device Structures" 34(10) (2009) 738.*

‡ *Moore, J. S.; Jones, K. S.; Kennel, H.; Corcoran, S., Ultramicroscopy "3-D Analysis of Semiconductor Dopant Distributions in a Patterned Structure using LEAP" (2008), 108, 536–539.*

CAMECA SCIENCE & METROLOGY SOLUTIONS

nu

AMETEK MATERIALS ANALYSIS DIVISION

CAMECA International Headquarters
29 quai des Grésillons
92622 Gennevilliers, France
cameca.info@ametek.com
www.cameca.com

Atom Probe Technology Center
5500 Nobel Drive
WI-53711 Madison, USA
cameca.leap@ametek.com
www.atomprobe.com